DOI: 10.2478/sspjce-2024-0003

Transient Flow in Pressurized Pipes: A Comparative Study of Five Resolution Methods

Abdelouaheb Toumi[1,2*], Fateh Sekiou[3,4], Fateh Afoufou[4,5]

[1]Laboratory of Civil Engineering and Hydraulics (LGCH), University of Guelma 8th May 1945, Guelma, Algeria.
[2]Department of Civil Engineering and Hydraulics (DGCH), University of Guelma 8th May 1945, Guelma, Algeria.
[3]Department of hydraulic, University of Oum El Bouaghi, Oum El Bouaghi, Algeria, sekiou.fateh@univ-oeb.dz
[4]Department of hydraulic, University of Batna 2, Batna, Algeria, f.afoufou@univ-batna2.dz
[5]LARHYSS Laboratory, Mohamed Khider University, Biskra, Algeria
*e-mail: toumi.abdelouaheb@univ-guelma.dz

Abstract

This article solves, models, and simulates, by five different methods, the system of partial differential equations of hyperbolic type governing the transient flow in the case of a gravity pipe supplied from a reservoir and equipped with a valve at its extremity. To make this work smoother and more attractive when calculating hydraulic parameters in transient flow, we took into consideration the two valve closing laws most commonly used in practice and in case of fast and slow closing. The reliability and safety of operation of the pressure pipeline system (PPS) depends on protection systems against the harmful effects of transient flow. To be able to place the most suitable protection device where it is needed, we must use numerical methods to model and simulate such processes. To this end, we applied five methods to solve the transient flow equations and subsequently search for the method giving results with practical credibility. The results obtained show that the methods of MarcCormak and Alternative lead, in fast and slow closures, to very close values by giving more logical graphic representations to the phenomenon generated. The Lax-Friedrichs method can join them but with another appearance of the representation of pressures, and the method of characteristics neglects certain parameters such as the inclination of the pipe while the Richtmayer method should be avoided in its current form because of the error gap between it and the other methods, and the graphical representation of the results obtained, like the pressure over time, which does not give a logical interpretation of the phenomenon produced.

Keywords: hyperbolic transient flow equations; resolution methods, most suitable method, pressurized pipes.

1 Introduction

In the networks of hydraulic systems, transient flows appear when the initial conditions of the permanent flow are disturbed, for example, in the case of the slow or fast closing of a valve. However, what is disturbing of these flows is the gigantic, in a lapse of time, of their parameters where their values exceed the tolerance. Several studies have been carried out on this subject of research such as Maurice Gariel's study on the optimization of closing law of distributor in order to reduce the water hammer and so codify the practical rules for calculating the maximum water hammer, and along a penstock supplying a turbine. Hayashi and Eansfoed's study of the sudden opening or closing of the valve downstream of a pipe [1], later Thirriot (1967) studied approximate methods for calculating water hammer in relatively long pipes [2]. Steeter et al (1983) and also Almeida and Koelle (1992) discuss the type of scheme that update when friction is dominant [3,4].

Zhang et al., (2018) studied unsteady flow friction model in coiled tubing [5] using an implicit finite difference method conducted by Twyman (2018) [6]. Trabelsi and Triki (2019) performed a dual control technique for mitigating water-hammer phenomenon in pressurized steel-piping systems [7]. Assessment of inline technique-based water hammer control strategy in water supply systems was highlighted by Ben Iffa and Triki (2019) and (Azhari et al., (2019) numerically analyzed the transient pressures in geothermal wells with water hammer during injection fall-off test [8,9]. Norazlina S. and Norsarahaida A. (2015) analyzed 6 types of valve closure laws: instantaneous (m=0), linear (m=1), concave (m=0.05), concave (m=0.5), convex (m=5) and convex (m=50), they clearly show the change in pressure wave profile and amplitude from one law to the other and notes that the instantaneous and convex closure law results in minimum and maximum pressure respectively [10]. Recently Zhao et al (2020) show that the flow rate and, in particular, the valve closing speed strongly affect the increase in water hammer pressure, the higher the flow rate and valve closing speed, the greater the increase in water hammer pressure [11]. Rahul and Arun (2020), who conducted experimental and numerical investigations of water hammer analysis in pipeline with two different materials and their combined configuration had been described [12]. In addition, Aliabadi et al., (2020) studied the frequency response of water hammer with fluid-structure interaction in a viscoelastic pipe [13]. In Mery et al., (2021) study, water hammer mitigation was carried out by air vessel and by pass forward configuration [14]. While Kandil et al., (2021) performed a study dealing with the effect of pipe materials properties on the water hammers by considering the fluid-structure interaction, frictionless model [15]. In addition, (Khalideh et al., 2021) investigated the influence of dimensions and material of the pipes on the water hammer effect in microbial fuel cells waste water treatment plants [16]. Sławomir (2021) applied the shock response spectrum method to severity assessment of water hammer loads [17]. Toumi and Remini (2021) solved the Saint Venant equations for cases of double and triple effect pumping stations [18]. Liu (2021) investigated the sensitivity of six main parameters that affect the transient flow rate, the results show that the flow rate and Young's modulus are positively correlated with the maximum pressure, while the pipe diameter, valve closing time and wall thickness are negatively correlated, he further states that the flow rate, diameter and valve closing time are the key parameters that affect the model simulation hammer [19].

Han et al (2022) showed that extending the valve closing time can effectively reduce the maximum water hammer pressure and that pressure vibration were affected by the closing law, the faster the valve closing speed in the closing early stage, the greater the water hammer pressure [20]. Cao et al (2022) notes that in both case of fast closing and slow closing situations, the optimized nonlinear valve closure presents different shapes this permit to guiding valve real-time control, as well as providing a reference for valve design for the purpose of wave surge [21].

This paper is devoted to the study of the transient flow of the hydraulic in gravity buried pipe, which consists of a cast iron pipe, specially optimize law and time closing valve. To achieve this objective, the calculation of water hammer will be based on the five numerical methods to calculate the hydraulic parameters in transient flow.

The search for the best calculation method among the five methods used requires numerous, meticulous, precise, repetitive and worrying calculations and demands extreme attention to the results obtained. In order to show how to carefully obtain this method, it is appropriate to show the general procedure to be followed through a case study.

2 Mathematical model

The equations can faithfully describe the phenomena of transient flow in hydraulic adduction pipeline are the basic hyperbolic equations demonstrated successively from the continuity equations and dynamics [3,18]:

$$\begin{cases} \rho\frac{\partial u}{\partial x}+\frac{1}{a^2}\left(\frac{\partial P}{\partial t}+u\frac{\partial P}{\partial x}\right)=0 \\ \frac{\partial u}{\partial t}+u\frac{\partial u}{\partial x}+\frac{1}{\rho}\frac{\partial P}{\partial x}=-g(\sin(\alpha)+j) \end{cases} \tag{1}$$

Where, a: wave velocity (m/s);
P: pressure (Pa);
ρ: density of the liquid, for water $\rho = 10^3 kg / m^3$;
u: velocity in the x direction (m/s);
g: acceleration due to gravity (m / s^2);
α: pipe inclination angle;
j: unit pressure drop.
These two equations express the variation of two parameters, namely velocity and pressure over time, t, in the direction of flow, x [22,23].To know the values of these two parameters at any time and in any place of a water supply pipeline, we used five methods to solve the mathematical model represented by the two previous partial differential equations. And since most of the data are given by flow and manometric pressure, we had to convert the two previous equations to these two parameters.

3 Transformation of the transient flow equations

The transformation of equations for transient flow in pressure pipes, written as a function of velocity and pressure (see system of equations 1), to equations written as a function of piezometric head and flow rate without neglecting the terms u(∂u/∂x) and u(∂P/∂x) in front of the terms ∂u/∂t and ∂P/∂t and the pipe may have an inclination with respect to the horizontal plane, i.e. sin(α)≠0, must use the following mathematical expressions and introduce them into the system equations number 1.

$$\frac{\partial P}{\partial t}=\frac{\partial(\rho g(H-Z)}{\partial t}=\rho g\left(\frac{\partial H}{\partial t}-\frac{\partial Z}{\partial t}\right) \tag{2}$$

Where : H and Z are successively the manometric head and the geodesic level.

$$\frac{\partial P}{\partial x} = \frac{\partial(\rho g(H-Z)}{\partial x} = \rho g\left(\frac{\partial H}{\partial x} - \frac{\partial Z}{\partial x}\right) \tag{3}$$

$$u\frac{\partial P}{\partial x} = \frac{Q}{S}\frac{\partial P}{\partial x} = \rho g\frac{Q}{S}\left(\frac{\partial H}{\partial x} - \frac{\partial Z}{\partial x}\right) \tag{4}$$

Where :S and Q are successively the pipe cross section and the flow rate.

$$\frac{\partial u}{\partial t} = \frac{1}{S}\frac{\partial Q}{\partial t} \tag{5}$$

$$u.\frac{\partial u}{\partial x} = \frac{Q}{S}\frac{\partial u}{\partial x} = \frac{Q}{S}\frac{1}{S}\frac{\partial Q}{\partial x} = \frac{Q}{S^2}\frac{\partial Q}{\partial x} \tag{6}$$

$$\frac{\partial u}{\partial x} = \frac{1}{S}\frac{\partial Q}{\partial x} \tag{7}$$

$$\begin{cases} a\left(\frac{1}{S}\frac{\partial Q}{\partial x}\right) + \frac{1}{\rho\, a}\left(\rho g\left(\frac{\partial H}{\partial t} - \frac{\partial Z}{\partial t}\right) + \rho g\frac{Q}{S}\left(\frac{\partial H}{\partial x} - \frac{\partial Z}{\partial x}\right)\right) = 0 \\ \frac{1}{S}\frac{\partial Q}{\partial t} + \frac{Q}{S^2}\frac{\partial Q}{\partial x} + \frac{1}{\rho}\left(\rho g\left(\frac{\partial H}{\partial x} - \frac{\partial Z}{\partial x}\right)\right) = -g(\sin(\alpha) + j) \end{cases} \tag{8}$$

$$\begin{cases} \left(\frac{a}{S}\frac{\partial Q}{\partial x}\right) + \frac{g}{a}\left(\left(\frac{\partial H}{\partial t} - \frac{\partial Z}{\partial t}\right) + \frac{Q}{S}\left(\frac{\partial H}{\partial x} - \frac{\partial Z}{\partial x}\right)\right) = 0 \\ \frac{1}{S}\frac{\partial Q}{\partial t} + \frac{Q}{S^2}\frac{\partial Q}{\partial x} + g\left(\left(\frac{\partial H}{\partial x} - \frac{\partial Z}{\partial x}\right)\right) = -g(\sin(\alpha) + j) \end{cases} \tag{9}$$

Multiply the first equation by a/g and the second by S, we get:

$$\begin{cases} \left(\frac{a^2}{gS}\frac{\partial Q}{\partial x}\right) + \left(\frac{\partial H}{\partial t} - \frac{\partial Z}{\partial t}\right) + \frac{Q}{S}\left(\frac{\partial H}{\partial x} - \frac{\partial Z}{\partial x}\right) = 0 \\ \frac{\partial Q}{\partial t} + \frac{Q}{S}\frac{\partial Q}{\partial x} + gS\left(\frac{\partial H}{\partial x} - \frac{\partial Z}{\partial x}\right) = -gS(\sin(\alpha) + j) \end{cases} \tag{10}$$

$$\begin{cases} \frac{\partial H}{\partial t} = \frac{Q}{S}\frac{\partial Z}{\partial x} - \left(\frac{a^2}{gS}\frac{\partial Q}{\partial x}\right) - \frac{Q}{S}\frac{\partial H}{\partial x} + \frac{\partial Z}{\partial t} \\ \frac{\partial Q}{\partial t} = -\frac{Q}{S}\frac{\partial Q}{\partial x} - gS\left(\frac{\partial H}{\partial x} - \frac{\partial Z}{\partial x}\right) - gS(\sin(\alpha) + j) \end{cases} \tag{11}$$

$\partial Z/\partial t=0$

$$\begin{cases} \frac{\partial H}{\partial t} = \frac{Q}{S}\frac{\partial Z}{\partial x} - \frac{a^2}{gS}\frac{\partial Q}{\partial x} - \frac{Q}{S}\frac{\partial H}{\partial x} \\ \frac{\partial Q}{\partial t} = -\frac{Q}{S}\frac{\partial Q}{\partial x} - gS\frac{\partial H}{\partial x} + gS\frac{\partial Z}{\partial x} - gS\sin(\alpha) - gSj \end{cases} \tag{12}$$

$\partial Z/\partial X=\sin(\alpha)$

$$\begin{cases} \frac{\partial H}{\partial t} = \frac{Q}{S}\sin(\alpha) - \frac{a^2}{gS}\frac{\partial Q}{\partial x} - \frac{Q}{S}\frac{\partial H}{\partial x} \\ \frac{\partial Q}{\partial t} = -\frac{Q}{S}\frac{\partial Q}{\partial x} - gS\frac{\partial H}{\partial x} - gSj \end{cases} \tag{13}$$

These two equations express the change in head and flow rate over time in the direction of flow. This transformation was carried out since in real cases, the data is available in heights and flows and all intermediate parameters are calculated by similar units.

4 Materials and methods

4.1 Solution methods

4.1.1 Method Of Characteristics

The application of the MOC on the system of equations number 1 gives the following algebraic expressions [19]:

$$\mathrm{CP} = \mathrm{H(i)} + \mathrm{RQ(i)} - \mathrm{T_1}.\left((\mathrm{Q(i+1)}.\,|\mathrm{Q(i)}|)\right) \tag{14}$$

$$\mathrm{CM} = \mathrm{H(i+2)} - \mathrm{RQ(i+2)} + \mathrm{T_1}.\left((\mathrm{Q(i+1)}.\,|\mathrm{Q(i+2)}|)\right) \tag{15}$$

$$\mathrm{H(i+1)} = (\mathrm{CP} + \mathrm{CM})/2 \tag{16}$$

$$\mathrm{Q(i+1)} = \big(\mathrm{CP} - \mathrm{H(i+1)}\big)/\mathrm{R} \tag{17}$$

These algebraic equations make it possible to calculate the flow rate and the manometric head in transient flow.

4.1.2 Lax-Friedrichs method

The Lax-Friedrichs method is used in this article to solve the transient flow equations mentioned in system number (13).This method makes it possible to transform the equations of the system number (13) into algebraic equations, easy to process numerically. Applying this scheme gives the following system of equations:

$$\begin{cases} \mathrm{H_i^{k+1}} = (\mathrm{H_{i+1}^k} + \mathrm{H_{i-1}^k})/2 + \mathrm{C_1} - \mathrm{C_2}\left(\mathrm{Q_{i+1}^k} - \mathrm{Q_{i-1}^k}\right) - \mathrm{C_3}\left(\mathrm{H_{i+1}^k} - \mathrm{H_{i-1}^k}\right) \\ \mathrm{Q_i^{k+1}} = (\mathrm{Q_{i+1}^k} + \mathrm{Q_{i-1}^k})/2 - \mathrm{d_1}(\mathrm{Q_{i+1}^k} - \mathrm{Q_{i-1}^k}) - \mathrm{d_2}(\mathrm{H_{i+1}^k} - \mathrm{H_{i-1}^k}) - \mathrm{d_3}\overline{\mathrm{Q}}_\mathrm{i}|\overline{\mathrm{Q}}_\mathrm{i}| \end{cases} \tag{17}$$

With :

$$\mathrm{C_1} = \frac{\overline{\mathrm{Q}}_\mathrm{i}\Delta \mathrm{t_i}\sin(\alpha)}{\mathrm{S}};\ \mathrm{C_2} = \frac{\mathrm{a^2}\Delta\mathrm{t}}{2\mathrm{gS}\Delta\mathrm{x}};\ \mathrm{C_3} = \frac{\overline{\mathrm{Q}}_\mathrm{i}\Delta\mathrm{t}}{2\mathrm{S}\Delta\mathrm{x}}$$

$$\mathrm{d_1} = \frac{\Delta\mathrm{t}}{2\Delta\mathrm{x}}\frac{\overline{\mathrm{Q}}_\mathrm{i}}{\mathrm{S}};\ \mathrm{d_2} = \frac{\Delta\mathrm{tgS}}{2\Delta\mathrm{x}};\ \mathrm{d_3} = \Delta\mathrm{t}\frac{\lambda}{2\mathrm{dS}}$$

$$\overline{\mathrm{Q}}_\mathrm{i} = \frac{1}{2}\left(\mathrm{Q_{i+1}^k} + \mathrm{Q_{i-1}^k}\right) \tag{19}$$

Δt: time step; Δx: space step; S: cross-section of the pipe; d: pipe diameter; λ: coefficient of friction; i: space index; k: time index.

4.1.3 Richtmayer method

This method is composed of two steps, one of prediction and the other of correction. The first step in the Richtmyer two-step Lax–Wendroff method calculates values for f(H(x, t)) and f(Q(x, t)) at half time steps, $t_{n+1/2}$ and half grid points, $x_{i+1/2}$. In the second step values at t_{n+1} are calculated using the data for t_n and $t_{n+1/2}$.

a. Predictor step

Application of the Richtmayer method for the first step on the system of equation number 13 gives the following expressions:

$$\begin{cases} H_{i1}^{k+1} = (H_{i+1}^{k} + H_{i}^{k})/2 + C_1 - C_2\left(Q_{i+1}^{k} - Q_{i}^{k}\right) - C_3\left(H_{i+1}^{k} - H_{i}^{k}\right) \\ H_{i2}^{k+1} = (H_{i}^{k} + H_{i-1}^{k})/2 + C_1 - C_2\left(Q_{i}^{k} - Q_{i-1}^{k}\right) - C_3\left(H_{i}^{k} - H_{i-1}^{k}\right) \\ Q_{i1}^{k+1} = (Q_{i+1}^{k} + Q_{i}^{k})/2 - d_1\left(Q_{i+1}^{k} - Q_{i}^{k}\right) - d_2\left(H_{i+1}^{k} - H_{i}^{k}\right) - d_3(\overline{Q}_i|\overline{Q}_i|) \\ Q_{i2}^{k+1} = (Q_{i}^{k} + Q_{i-1}^{k})/2 - d_1\left(Q_{i}^{k} - Q_{i-1}^{k}\right) - d_2\left(H_{i}^{k} - H_{i-1}^{k}\right) - d_3(\overline{Q}_i|\overline{Q}_i|) \end{cases} \tag{20}$$

With :

$$C_1 = \frac{\overline{Q}_i \Delta t_i \sin(\alpha)}{S};\ C_2 = \frac{a^2 \Delta t}{2gS\Delta x};C_3 = \frac{\overline{Q}_i \Delta t}{2S\Delta x}$$

$$d_1 = \frac{\Delta t}{2\Delta x}\frac{\overline{Q}_i}{S};d_2 = \frac{\Delta tgS}{2\Delta x};\ d_3 = \Delta t\frac{\lambda}{2dS}$$
$$\overline{Q}_i = \frac{1}{2}(Q_{i+1}^{n} + Q_{i-1}^{n})$$

b. Corrector step

Applying the second step, gives the following expressions:

$$\begin{cases} H_{i}^{k+1} = H_{i}^{k} + C_{11} - C_{22}\left(Q_{i1}^{k} - Q_{i2}^{k}\right) - C_{33}\left(H_{i1}^{k} - H_{i2}^{k}\right) \\ Q_{i1}^{k+1} = Q_{i}^{k} - d_{11}\left(Q_{i1}^{k} - Q_{i2}^{k}\right) - d_{22}\left(H_{i1}^{k} - H_{i2}^{k}\right) - d_{33}(\overline{Q}_i|\overline{Q}_i|) \end{cases} \tag{21}$$

With:

$$C_{11} = C1; C_{22} = 2C_2; C_{33} = 2C_3$$
$$d_{11} = 2d_1; d_{22} = 2d_2; d_{33} = d_3$$

4.1.4 MacCormak method

The MacCormack method is a widely used discretization scheme for the numerical solution of hyperbolic partial differential equations. This second-order finite difference method was introduced by Robert W. MacCormack in 1969 [24]. The MacCormack method is elegant and easy to understand and program [25].

a. Predictor step

In the predictor step, the provisional values of H and Q at time level (t+Δt) are estimated as follows:

$$\begin{cases} H_i^* = H_i^k + C_1 - C_2\left(Q_{i+1}^k - Q_i^k\right) - C_3\left(H_{i+1}^k - H_i^k\right) \\ Q_i^* = Q_i^k - d_1\left(Q_{i+1}^k - Q_i^k\right) - d_2\left(H_{i+1}^k - H_i^k\right) - d_3\overline{Q}_i|\overline{Q}_i| \end{cases} \quad (22)$$

With:

$$C_1 = \frac{\overline{Q}_i \Delta t_i \sin(\alpha)}{S}; C_2 = \frac{a^2 \Delta t}{gS\Delta x}; C_3 = \frac{\overline{Q}_i \Delta t}{S\Delta x}$$

$$d_1 = \frac{\Delta t}{\Delta x}\frac{\overline{Q}_i}{S}; d_2 = \frac{\Delta tgS}{\Delta x}; \ d_3 = \Delta t\frac{\lambda}{2dS}$$

b. Corrector step

In the corrector step, the predicted values H and Q are corrected according to the follow equations :

$$\begin{cases} H_i^{k+1} = (H_i^k + H_i^*)/2 + C11 - C22\left(Q_i^k - Q_{i-1}^k\right) - C33\left(H_i^k - H_{i-1}^k\right) \\ Q_i^{k+1} = (Q_i^k + Q_i^*)/2 - d11\left(Q_i^k - Q_{i-1}^k\right) - d22\left(H_i^k - H_{i-1}^k\right) - d33\overline{Q}_i|\overline{Q}_i| \end{cases} \quad (23)$$

With:

$$C_{11} = \frac{\Delta t\overline{Q}_i}{S}\sin(\alpha); C_{22} = \frac{\Delta ta^2}{2gS\Delta x}; C_{33} = \frac{\Delta t\overline{Q}_i}{S2\Delta x}$$

$$d_{11} = \frac{\Delta t\overline{Q}_i}{2\Delta xS}; d_{22} = \frac{\Delta tgS}{2\Delta x}; d_{33} = \frac{\Delta t\lambda}{2dS}$$

4.1.5 Alternative method

Like the methods of Richtmayer and MarcCormak, the alternative method consists of two steps, the first for the prediction and the second for the correction.

a. Predictor step

$$\begin{cases} H_{i1}^{k+1} = H_i^k + C_1 - C_2\left(Q_i^k - Q_{i-1}^k\right) - C_3\left(H_i^k - H_{i-1}^k\right) \\ Q_{i1}^{k+1} = Q_i^k - d_1\left(Q_i^k - Q_{i-1}^k\right) - d_2\left(H_i^k - H_{i-1}^k\right) - d_3\overline{Q}_i|\overline{Q}_i| \end{cases} \quad (24)$$

With:

$$C_1 = \frac{\overline{Q}_i \Delta t_i \sin(\alpha)}{S}; \ C_2 = \frac{a^2 \Delta t}{gS\Delta x}; \ C_3 = \frac{\overline{Q}_i \Delta t}{S\Delta x}$$

$$d_1 = \frac{\Delta t}{\Delta x}\frac{\overline{Q}_i}{S}; \ d_2 = \frac{\Delta tgS}{\Delta x}; \ d_3 = \Delta t\frac{\lambda}{2dS}$$

b. Corrector step

$$\begin{cases} H_{i1}^{k+1} = \frac{1}{2}\left(H_i^k + H_{i1}^{k+1}\right) + C_{11} - C_{22}\left(Q_{i+1}^{k+1} - Q_i^{k+1}\right) - C_{33}\left(H_{i+1}^{k+1} - H_i^{k+1}\right) \\ Q_{i1}^{k+1} = \frac{1}{2}\left(Q_i^k + Q_{i1}^{k+1}\right) - d_1\left(Q_{i+1}^{k+1} - Q_i^{k+1}\right) - d_2\left(H_{i+1}^{k+1} - H_i^{k+1}\right) - d_3\overline{Q}_i|\overline{Q}_i| \end{cases} \quad (25)$$

With:

$$C_{11} = C_1 = \frac{\overline{Q}_i \Delta t_i \sin(\alpha)}{S}; C_{22} = C_2/2 = \frac{a^2 \Delta t}{2gS\Delta x}; \ C_{33} = C_3/2 = \frac{\overline{Q}_i \Delta t}{2S\Delta x}$$

$$d_{11} = d_1/2 = \frac{\Delta t}{2\Delta x}\frac{\overline{Q}_i}{S};\ d_{22} = d_2/2 = \frac{\Delta t g S}{2\Delta x}; d_{33} = d_3 = \Delta t\frac{\lambda}{2dS}$$

4.2 Problem statement and boundary conditions

4.2.1 Problem statement

To give concrete form to the mathematical model obtained and put into practice the five resolution methods, the RPV (Reservoir - Pipeline - Valve) system is adopted: it consists of a large reservoir at the upstream end of the inclined pipeline and a valve at the downstream end discharging to the atmosphere. A reservoir (R) equipped with an overflow at an altitude of 200 m, supplies a flow of 350 l/s via a gravity pipe (P) of length equal to 1000 m and inclined at 10°. The motorized valve with controlled closure is located at the other end of the pipe, at an altitude of 50 m. The transient flow is generated by fast and/or slow valve closing time. The schematic shape of the problem is shown in Fig 1.

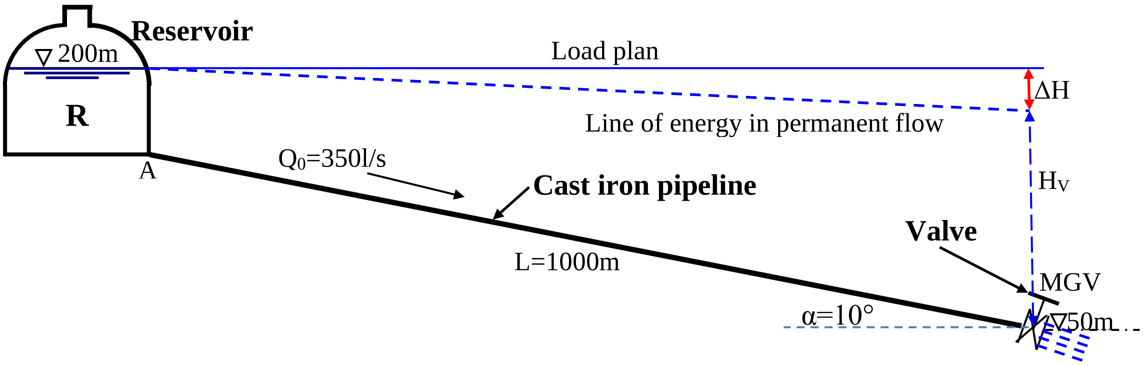

Figure 1: Schematic of the reservoir-pipe-valve system

4.2.2 Boundary conditions and stability criterion

When applying the MOC, Lax–Friedrichs, Richtmayer, MacCormak and Alternative methods, they appear, at the limits (on the left and on the right), undefined variables in the domain of interest, this section has highlighted how we get rid of -us definitely.

a. At the outlet of the reservoir

The manometric head at the level of the first node (inlet of the pipe) is equal to the manometric height of the water in the reservoir H(1)=Hr, while the flow rate is obtained by applying the characteristic equations on the left and its expression is written as follows.

$$CN = H(2) - Q(2)(R - T.|Q(2)|) \tag{26}$$

H(2) and Q(2) are quantities calculated at time (t) so:

$$Q(1) = (H_R - CN)/R \tag{27}$$

With:

$$T = B.(x(i+2)-x(i+1)) = B.\Delta x \tag{28}$$

$$B = \frac{\lambda}{2.g.d.S^2} \tag{29}$$

And

$$R = \frac{a}{g.S} \tag{30}$$

Where: the parameter R represents the flow resistance effect and the elements of this parameter are: a: wave velocity (m/s); S: pipe cross section in (m^2).

b. At the valve

In the case of instantaneous closing (valve closing time equals zero) Q(n)=0, the manometric head at node number N is written as follows:

$$H(n) = CP \tag{31}$$

With:

$$CP = H(n-1) + Q(n-1)(R - T.|Q(n-1)|) \tag{32}$$

In the case where closing is controlled, the flow at the valve follows, over time, a function depending on the chosen closing law, and the flow, in this case, is written as a function of Q0, Δt, Ct and m by the following expression [10,26].

$$Q_n^{k+1} = \left(1 - \left(\frac{i\Delta t}{Ct}\right)^m\right) Q_n^k \tag{33}$$

Where,
m : exponent determining the valve closing law;
Δt: time step;
k: time index;
Ct: the total valve closing time;
Q^K and Q^{K+1} are successively the flow rates at times t and t+Δt.
Figure hereafter shows the envelope curves of the possible laws for closing a valve in a hydraulic system.

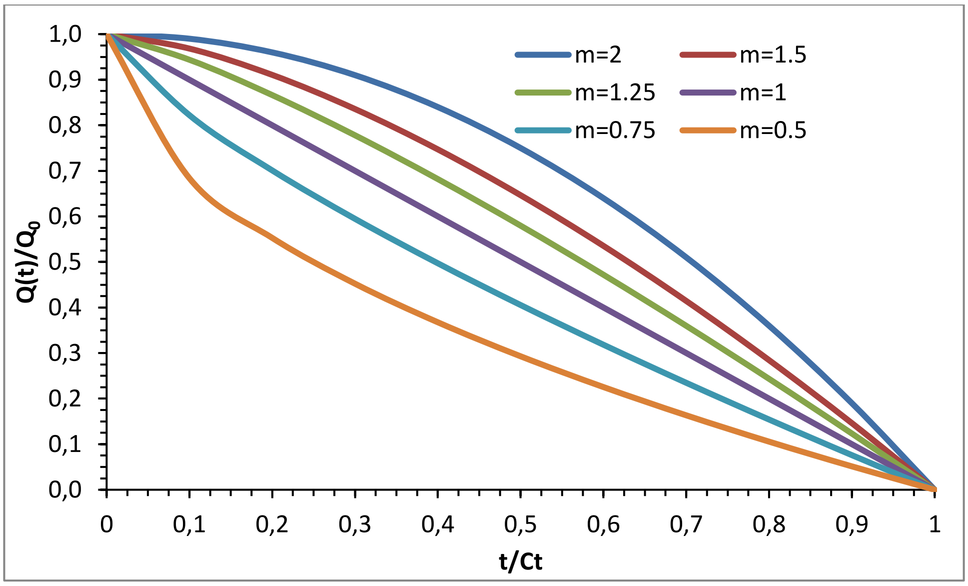

Figure 2: Closing functions corresponding to different values of exponent m

The exponent m, of the expression of Q at node n, generates the infinity of functions of Q and consequently the search for the optimal value of this exponent turns out to be a major priority for an optimal management.
In this case, the manometric head at the valve is calculated by the following relationship:

$$H(n) = CP - R.Q(n) \tag{34}$$

With:

$$CP = H(n-1) + Q(n-1)(R - T.|Q(n-1)|) \tag{35}$$

The stability criterion of the Lax method must ensure the stability of the finite difference method and the method of characteristics (MOC), which allows us to write the following expression:

$$\Delta x \geq a.\Delta t \tag{36}$$

Where, a: wave velocity in (m/s); Δt: time step; Δx: space step; N: number of discretization nodes; L: length of the pipe [6, 27, 28].
The flowchart in Figure 3 gives the schematic representation of the solution to the transient flow problem in pressurized pipelines.

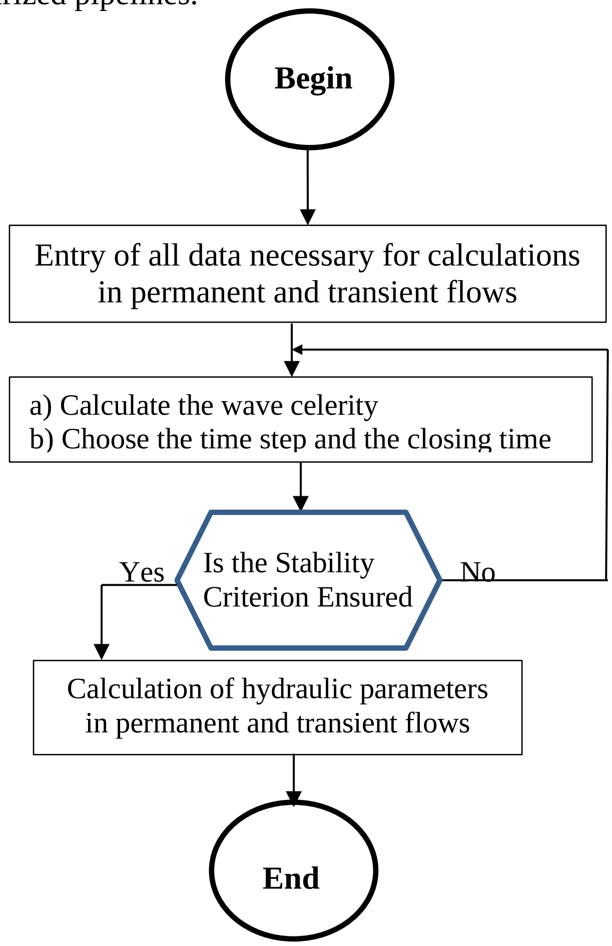

Figure 3: Flowchart for calculating hydraulic parameters in transient state

The execution of this algorithm requires knowledge of the characteristics of the materials used, the reservoir, the volume flow transported by the pipe and the liquid. All the latter characteristics are represented in table 1.

Table 1: Information regarding the proposed problem and used methods

Kind of materials	Cast iron
Elasticity modulus in Pascal	E_{FC}=1.03. 10^{11}
Pipe Poisson's ratio	ν_m= 0.26
Coefficient of vertical friction between the backfill and the walls of the trench	μ'=0.50
Rankine's coefficient	K=0.33
Soil density (KN/m^3)	γ=19000
Height of embankment above pipe (H) in (m)	1.0 m
Trench width (B_d) in (m)	1.10 m
exterior diameter (B_C)in (mm)	d_{ext}=635
internal diameter in (mm)	d_{int}=600
Pipe thickness e_1 in (mm)	e_1=17.5
Pipe roughness ε in (mm)	ε=0.03
Pipe length (m)	L=1000
Pipe inclination	10°
Pipe pressure rating in (bar)	42
Fluid elasticity modulus	Kw = 2.07.10^9 Pa
Fluid temperature	15°C
Kinematic viscosity	1.1445. 10^{-6} (m^2/s)
Density of the liquid	ρ = 10^3kg/m^3
Reservoir overflow level in (m)	200
Flow leaving the reservoir in (l/s)	350
Initial rapid valve closure time	0,01 t_4 seconds
Final rapid valve closure time	0,5 t_4 (t_4 return period)
Initial slow valve closure time	0,51 t_4
Final slow valve closure time	10 t_4
MOC, Lax-Friedrichs, Richtmayer, MacCormak and Alternative	one-dimensional

5 Results and Discussion

To begin transient calculations, the resolution method has to use the results obtained under steady-state conditions. The results are shown in Table 2.
Instantaneous closure (zero closure time) generates an oscillatory phenomenon of overpressure and underpressure with a return period of 4L/a Dupont A., (1979), which has harmful effects on the pipe and its appurtenances at the same time. Although practically unfeasible due to its zero delay, this type of closure must be avoided if the hydraulic system is not to be jeopardized[29]. In addition, it generates high pressures which, at certain points in the hydraulic system, exceed the resistance of the pipe. Whereas rapid closing, with a closing time of between

0 and 0.5 t_4 (where t4 is the return period) Dupont A., (1979), generates high pressure values which can also damage the hydraulic system [29]. Closing is said to be slow if the valve's closing time is greater than the shock wave's forward and return times t >$0.5t_4$ [29]. Manual closing is not mandatory. Indeed, technological advances have led to the emergence of motorized valves that close and open according to the control signal. This opportunity generates laws linking flow and control signal, such as linear, concave and convex laws. From the first operation at $t=t_0$ (t_0 is the equilibrium time) until the valve is completely closed, and after a certain time after closure, what will be the values of the flow parameters at all the nodal points in the pipe. The answer to this question is part of what follows.

Table 2: Simulation result in steady state

Average flow velocity V in (m/s)	1.2378
Reynolds number Re	648933.500
coefficient of friction Lambda	$1.334596\ 10^{-2}$
Load loss in (m)	1.9109
Number of discretization points N	892
Duration of the return period t_4 in (seconds)	3.564
The value of R=a/gS in (s/m^2)	404.632507
Water hammer value Vdh in (m)	141.621384
Pipe resistance RC in (s^2/m^5)	15.599385
The space step Δx in(m)	1.1223
the time step Δt in (s)	0.001
Resistance of the discretization element RDE in (s^2/m^5)	$1.75.10^{-2}$
Manometric head in (m)	198.089081
Manometric pressure in (m.w.c)	148.089081
Pressure in (bar)	14.527

5.1 Case of rapid valve closing

To determine the effect of rapid closure on overpressure values for linear and quadratic laws, we simulated valve pressure for times ranging from 0.01 t_4 to 0.5 t_4 with a time step of 0.01 t_4(i.e. 50 valve closing times tested).Figures 4 and 5 show successively for linear and quadratic valve closing laws, the evolution of the overpressure as a function of time at the valve for the five closing methods tested.

These graphic representations lead to different physical interpretations of the phenomenon. Indeed, the Richtmayer method records the largest value of pressure at the start of the calculation and this value decreases linearly over time. The MOC shows that during this interval, the pressure increases proportionally during the time of the wave's outward and return journey. The Lax method records arising pressure which is characterized by the appearance of two lines of different slopes. The high slope line (lower) is linked to the direction of the wave from the valve to the reservoir (from t_0=0.01 to t_1=L/a) and the lows lope line (upper) is linked to the return of the wave from the tank to the valve (from t_1=L/a to t_2=2L/a). The graphs of the MacCormak and Alternative methods are both characterized by the appearance of two straight lines, the first rising specific to the time of the wave from the valve to the reservoir (from t_0=0.01 to t_1=L/a) and the second descending specific to the return time of the wave from the tank to the valve (from t_1=L/a to t_2=2L/a).

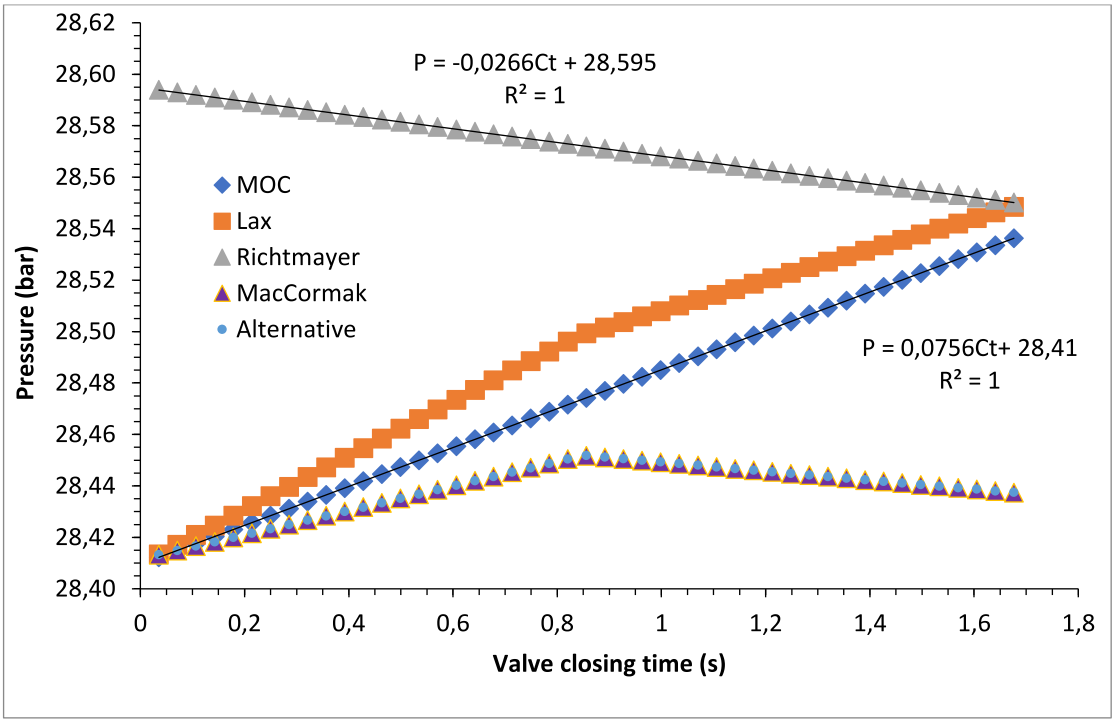

Figure 4: Variation of pressure for linear closing law as a function of time closing valve for the cast iron pipeline

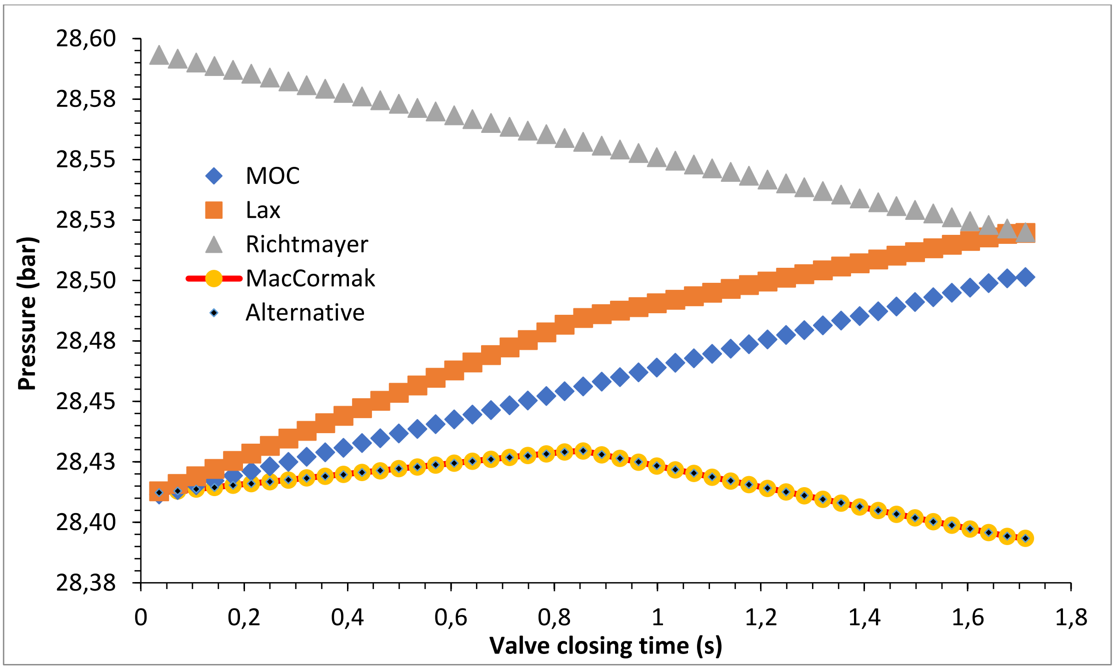

Figure 5: Variation of pressure for quadratic closing law as a function of time closing valve for the Cast iron pipeline

5.2 Case of slow valve closing

This section is focused on the search, for different valve closing times t ranging from 0.01 t_4 seconds to 10 t_4 seconds (i.e. 950 valve closing times tested), with a step size of Δt=0.001s, for the for linear and quadratic closing laws generating the overpressure and the underpressure.
Figures 6, 7, 8 and 9 show respectively the variation over time (t equal to 10 t_4) of the overpressure and depression at the valve for a slow closing time equal to twice the return period (2 t_4) for the valve closing laws linear and quadratic.

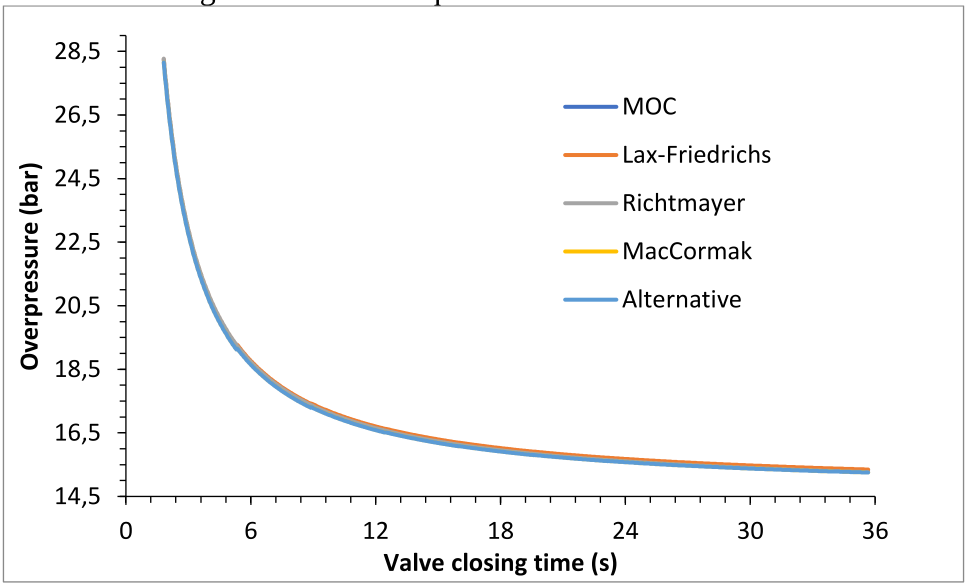

Figure 6: Variation of overpressure for linear closing laws (m=1) as a function of time closing valve for the cast iron pipeline

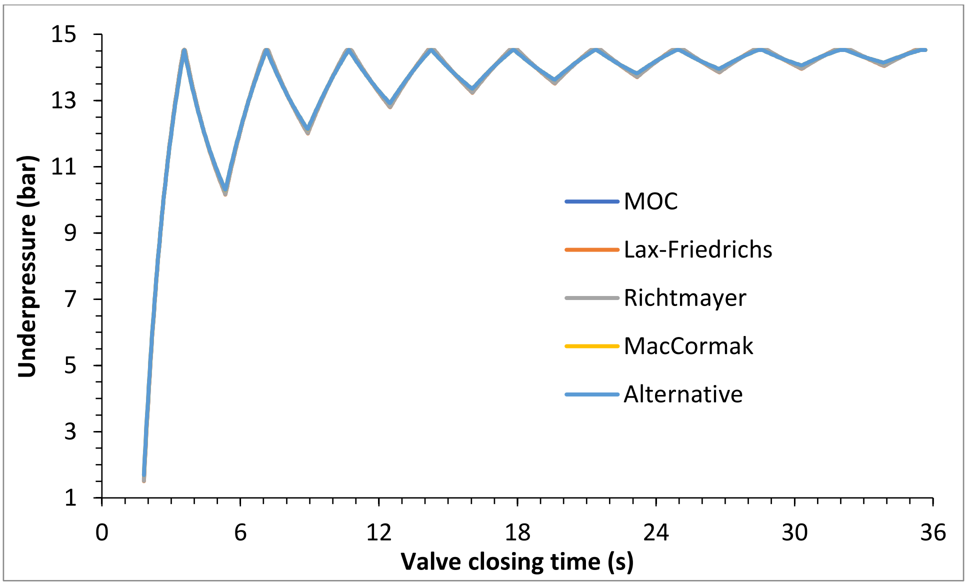

Figure 7: Variation of underpressure for linear closing laws (m=1) as a function of time closing valve for the cast iron pipeline

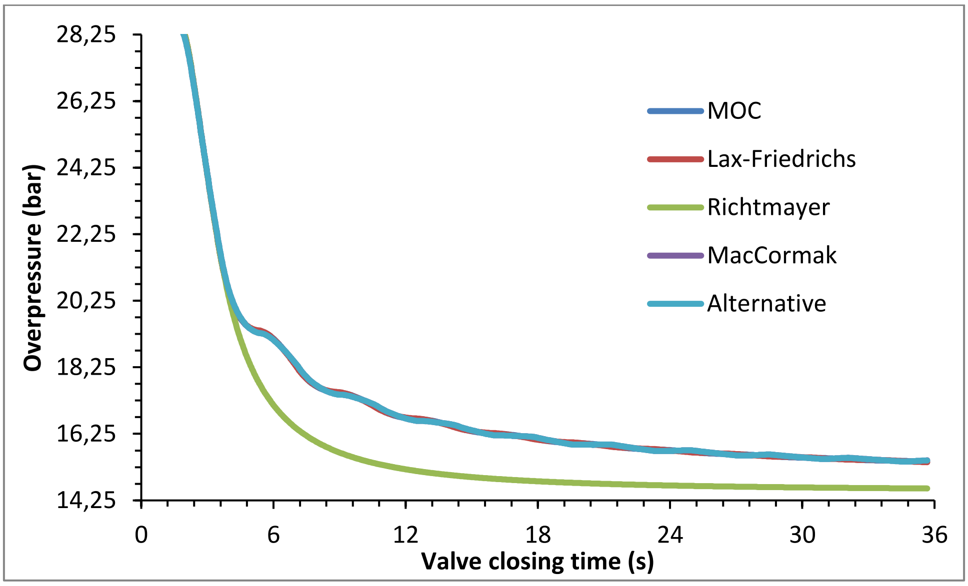

Figure 8: Variation of overpressure for quadratic closing laws (m=2) as a function of time closing valve for the cast iron pipeline

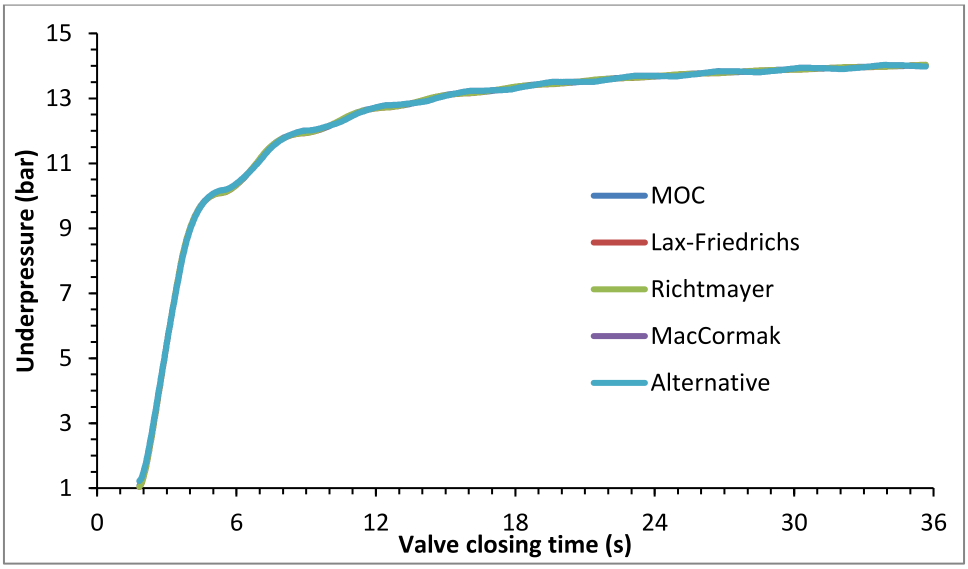

Figure 9: Variation of underpressure for quadratic closing laws (m=2) as a function of time closing valve for the cast iron pipeline

When the valve closing law takes a linear form, the five methods give overpressure and depression curves which converge almost in the same way to stabilize at the permanent state values. While the quadratic law of closing the valve shows that the Richtmayer method, in the case of calculating the overpressure, gives beyond a time approximately equal to t=4.20 seconds a curve distinct from the others while the curves of depression almost coincide.

6 Conclusion

In this paper, five methods have been used to solve the system of hyperbolic equations in partial derivatives governing transient flow in hydraulic systems under pressure. The search for a reliable method, giving reasonable results with a logical interpretation of the physical phenome nongenerated, requires the application of these five techniques. A transient flow is reproduced by the linear and quadratic closing of a valve placed in a simple hydraulic system composed of a reservoir, a pipe, and a valve.
The application of the five methods to the cases of fast and slow closures shows that the two methods of MarcCormak and Alternative lead, in fast and slow closures, to very close values by giving graphic representations allowing more logical interpretations of the phenomenon physics generated. The Lax-Friedrichs method can also be considered useful but with another appearance of the representation of the pressures and another philosophy of the interpretation of the results obtained. The method of characteristics neglects certain parameters like the inclination of the pipe but it remains useful at the limits to make start other methods while the Richtmayer method should be avoided in its current form given the error gap between it and the other methods and the unique appearance that it gives to the graphic representation of the variation of the overpressure over time.

References

[1] Hayashi T., Eansfoad G. (1960). Sudden opening or closing of an outlet valve on a pipeline, revue la Houille Blanche. N° 6, pp. 657-673.

[2] Thirriot C. (1967). Méthodes approchées de calcul des coups de bélier dans des conduits relativement longues, La Houille Blanche. N°2, pp. 179–192.

[3] Streeter V. L., Wylie E. B. (1983). Fluid Mechanics, 206 pages. Eds. McGraw-Hill, Ryerson Ann Arbor. Michigan 48106 U.S.A.

[4] Almeida A., Koelle E. (1992). Fluid Transients in Pipe Networks, *Computational Mechanics Publications and Elsevier Applied Science*. 564 pages

[5] Wenping Z., Huaizhong S, Gensheng li, Xianzhi S. (2018), Fluid hammer analysis with unsteady flow friction model in coiled tubing drilling, *Journal of Petroleum Science and Engineering PII*: S0920-4105(18)30274-2, DOI: 10.1016/j.petrol.2018.03.088

[6] Twyman J. (2018). Interpolation schemes for valve closure modelling, *Ingeniare: Revista Chilena de Ingenieria*. N°26, pp. 252–263.

[7] Trabelsi M., Triki A. (2019), Dual control technique for mitigating water-hammer phenomenon in pressurized steel-piping systems, International, *Journal of Pressure Vessels and Piping* N°172, pp. 397–413.

[8] BenIffa R., Triki A. (2019), Assessment of inline technique-based water hammer control strategy in water supply systems, Journal of Water Supply: *Research and Technology-Aqua*. Vol 68, Issue 7, pp. 562–572.

[9] Aazhari S. Adiputro, Sadiq J. Zarrouk, Richard J. Clarke, Virginie Harcouët-Menou, STIJN Bos (2020), Geothermal wellswith water hammer during injection fall-off test: Numerical pressure transient analysis, Geothermics, Vol 87, pp. 1-12.

https://doi.org/10.1016/j.geothermics.2020.101838

[10] SUBANI N., NORSARAHAIDA A. (2015). Analysis of water hammer with different closing valve laws on transient flow of hydrogen-natural gas mixture, *Abstract and Applied Analysis*. Volume, Article ID 510675, 12 pages.

[11] Li Zhao,Yusi Yang, Tong Wang, Wensheng Han, Rongchu Wu,Pengli Wang,Qiaoning Wang, and Liang Zhou(2020), An Experimental Study on the Water Hammer with Cavity Collapse under Multiple Interruptions, *Water* 2020, *12*(9), 2566;

https://doi.org/10.3390/w12092566

[12] Rahul K. G., Arun K. (2020), Experimental and numerical investigations of water hammer analysis in pipeline with two different materials and their combined configuration, *International Journal of Pressure Vessels and Piping*, Vol.188, 104219, pp.1-11.

[13] Aliabadi H. K., Ahmadi A., Keramat A.R. (2020),Frequency response of water hammer with fluid-structure interaction in a viscoelastic pipe, *Mechanical Systems and Signal Processing*, Vol 144, pp.1-19. https://doi.org/10.1016/j.ymssp.2020.106848

[14] Mery H. O., Hassan J. M., Ekaid A. L. (2021), Water Hammer Mitigation by Air Vessel and By pass Forward Configuration, IOP Conf. Series: *Materials Science and Engineering*, pp. 1-16. doi:10.1088/1757-899X/1094/1/012052

[15] Kandil M., Kamal A.M., El-Sayed T.A. (2021), Study the effect of pipe materials properties on the water hammer considering the fluid-structure interaction, frictionless model, *International Journal of Pressure Vessels and Piping*.

https://doi.org/10.1016/j.ijpvp.2021.104550.

[16] Khalideh Al. Bk. Al., La'Aly A. Al-S., Abeer Al-B., Alessa A., Amani Ly., EID Gul., Zhou H., Qing Y., Pietro B., Francesco F. (2021), Investigation of the influence of dimensions and material of the pipes on the water hammer effect in microbial fuel cells wastewater treatment plants, *Sustainable Energy Technologies and Assessments*, Vol 44, pp. 1-10.

[17] Sławomir H. (2021), Applied the shock response spectrum method to severity assessment of water hammer loads, *Mechanical Systems and Signal Processing*, Vol 157, , pp. 1-15.

[18] Toumi A., Remini B. (2022), Resolution of the Saint-Venant equations: a case of double and triple effect pumping stations, *Arabian Journal of Geosciences*, pp.1-23.

https://doi.org/10.1007/s12517-021-08269-8

[19] Jinhao Liu Jianhua Wu, Yusheng Zhang, Xinhao Wu (2021), Sensitivity Analysis of Hydraulic Transient Simulations Based on the MOC in the Gravity Flow, *Water* 2021, *13*(23), 3464; https://doi.org/10.3390/w13233464

[20] Yong Han, Weidong Shi, Hong Xu, Jiabin Wang, and Ling Zhou(2022), Effects of Closing Times and Laws on Water Hammer in a Ball Valve Pipeline, *Water* 2022, *14*(9), 1497 https://doi.org/10.3390/w14091497;

[21] Zheng Cao,Qi Xia,Xijian Guo,Lin Lu, and Jianqiang Deng(2022) A Novel Surge Damping Method for Hydraulic Transients with Operating Pump Using an Optimized Valve Control Strategy, *Water* 2022, *14*(10), 1576; https://doi.org/10.3390/w14101576

[22] Meunier M. (1980). Les coups de bélier et la protection des réseaux d'eau sous pression, in: *ENGREF*, Paris, 198 pages.

[23] Oouargh Y. (1971). Ecoulement forcé en hydraulique, Tome II, *Édition Paris*.

[24] MacCormack, R. W., The Effect of viscosity in hypervelocity impact cratering, *AIAA Paper*, 69-354 (1969).

[25] Anderson, J. D., Jr., Computational Fluid Dynamics: The Basics with Applications, *McGraw Hill* (1994)

[26] Provenzano P.G., Baroni F., Aguerre R. J. (2011). The closing function in the water hammer modeling, Latin American Applied Research. Vol. 41, pp. 43–47.

[27] Shamine L.F(2005) Two-step Lax–Friedrichs method, *Applied Mathematics Letters* 18 1134–1136

[28] Goldberg D. E., BENJAMIN W. E. (1983). Characteristics method using time-line interpolations, *Journal of Hydraulic Engineering*. N°109, pp. 670–683.

[29] Dupont A. (1979). Hydraulique urbaine, ouvrages de transport – Elévation et distribution des eaux. Tome 2. *Edition Eyrolles* Paris. 484 pages.